

## THE CONSTRUCTION OF ZONAL MODELS OF DISPERSION IN CHANNELS VIA MATCHED CENTRE MANIFOLDS

S. D. WATT<sup>1</sup> and A. J. ROBERTS<sup>2</sup>

(Received 17 June 1994; revised 31 January 1995)

### Abstract

Taylor's model of dispersion simply describes the long-term spread of material along a pipe, channel or river. However, often we need multi-mode models to resolve finer details in space and time. Here we construct zonal models of dispersion *via* the new principle of matching their long-term evolution with that of the original problem. Using centre manifold techniques this is done straightforwardly and systematically. Furthermore, this approach provides correct initial and boundary conditions for the zonal models. We expect the proposed principle of matched centre manifold evolution to be useful in a wide range of modelling problems.

### 1. Introduction

This paper is an exploration and development of the principle of matched centre manifolds in constructing low-dimensional models of dynamical systems. By using the well-studied example of shear dispersion in pipes and channels, we demonstrate the utility of the new principle.

G. I. Taylor [14] considered the dispersion of contaminant in a pipe. He derived an advection-diffusion model for the longitudinal transport and dispersion. This model predicts a transport of contaminant with the average velocity and with an effective diffusivity depending on the velocity profile and cross-pipe diffusivity. Since then there have been a variety of approaches to analysing dispersion, for example [13, 4, 6]. There have also been several studies [7, 15, 8] using centre manifold theory to derive such low-dimensional models of the dispersion; the basics are summarised in Section 1.1. Centre manifold theory usefully provides these models with initial and boundary conditions, and also caters for the presence of spatial and temporal variations in the flow.

<sup>1</sup>Dept of Maths, University of Melbourne, Parkville, Vic. 3052, Australia.

<sup>2</sup>Dept of Maths & Comp., University of Southern Queensland, Toowoomba, Qld. 4350, Australia.

© Australian Mathematical Society, 1996, Serial-fee code 0334-2700/96

However, there are difficulties encountered in using these results to predict contaminant dispersion. These problems include restricted spatial resolution, limited transient predictions and difficulties in coding high order derivatives (especially in the boundary conditions). Many of these problems are at least partially overcome by using an invariant manifold approach (see [15]) but such analysis is considerably more difficult, especially for boundary conditions and for nonlinear problems.

In this paper, we show how to overcome some of the difficulties. In Section 2 we construct models of shear dispersion by requiring that a model has the “same” centre manifold evolution, to some order, as that for the original problem. This method of matching centre manifolds is a new notion in the low-dimensional modelling of dynamical systems. (In some ways it is similar to the idea of embedding a centre manifold, as discussed in [12].) In this application the constructed models may be called zonal as we identify a mode of slow advection with the near bank zone, and a mode of fast advection with the mid-stream zone.

Recently Chickwendu *et al.* [4] heuristically developed a similar zonal model of dispersion in rivers and channels; the model involved a mode to model the “slow zone” near the banks and bed, and a mode to model the “fast zone” in the channel centre. However, a difference is that here the parameters of the model are determined systematically *via* centre manifold theory.

Furthermore, to construct a complete model we also need initial and boundary conditions to supplement the evolution equation of the zonal model. Appropriate initial conditions of the zonal model, given the initial conditions of the original system, are found in Section 3 by matching the initial conditions of both centre manifolds. Techniques described by Roberts [10] give these initial conditions. Similarly, boundary conditions for the centre manifold models, obtained using techniques described in Roberts [12], are matched in Section 4 to provide correct inlet and outlet boundary conditions for the zonal model.

Thus this principle of matched centre manifolds systematically generates models of arbitrary order complete with initial and boundary conditions.

**1.1. The centre manifold of channel dispersion** As a prelude to this exploratory work, we here summarise the most basic centre manifold model of shear dispersion in a channel.

Consider the flow of a contaminant in a channel of constant width, modelled by the advection-diffusion equation

$$\frac{\partial c}{\partial t} + \nabla \cdot (\mathbf{q}c) = \nabla \cdot (\kappa \nabla c),$$

where  $c$  is the concentration of the contaminant,  $\mathbf{q}$  is the advection velocity and  $\kappa$  is the constant diffusivity. No flux of contaminant through the banks of the river requires that  $\partial c / \partial y = 0$  at  $y = \pm b$ , where  $b$  is the half-channel width.

We assume that the fluid is incompressible and the advection is along the channel (the  $x$ -direction) according to the velocity profile

$$\mathbf{q} = i\mathbf{u}(y) = i\frac{3}{2}U \left(1 - \frac{y^2}{b^2}\right),$$

where  $U$  is the average velocity. As noted many times, see [15] for example, downstream diffusion can be neglected without affecting more than a few minor details. Doing this,  $x$  and  $y$  can be rescaled independently,  $y$  with respect to  $b$  and  $x$  with respect to  $Ub^2/\kappa$ , so that in effect  $\kappa = 1$  and  $U = 1$ . Thus the nondimensional equation to analyse is

$$\frac{\partial c}{\partial t} + \frac{3}{2}(1 - y^2)\frac{\partial c}{\partial x} = \frac{\partial^2 c}{\partial y^2}. \tag{1}$$

As the cross-stream diffusion operator  $\partial^2/\partial y^2$  has one neutral mode and all other modes decay, centre manifold techniques may be applied to analyse the long-term behaviour of this system (as explained more fully by Mercer and Roberts [7]). The analysis is valid when the longitudinal gradients,  $\partial/\partial x$ , are small. Centre manifold theory [2] assures us that the system (1) evolves exponentially quickly to a low-dimensional state which is dominated by the neutral mode. The system then evolves slowly. To describe this low-dimensional, long-term evolution Mercer and Roberts [7] assume that the system is dependent only on this neutral mode, say

$$c = V(y, C) \quad \text{such that} \quad \frac{\partial C}{\partial t} = G(C), \tag{2}$$

where  $C(x, t)$  is defined to be the cross-stream average of  $c(x, y, t)$  and is therefore a measure of the ‘‘amplitude’’ of the neutral mode.

Mercer and Roberts then developed asymptotic expansions

$$V \sim \sum_{n=0}^{\infty} v_n(y) \frac{\partial^n C}{\partial x^n} \quad \text{and} \quad G \sim \sum_{n=1}^{\infty} g_n \frac{\partial^n C}{\partial x^n} \tag{3}$$

for these quantities where, for example,

$$v_0(y) = 1, \tag{4}$$

$$g_1 = -1, \tag{5}$$

$$v_1(y) = -(15y^4 - 30y^2 + 7)/120, \tag{6}$$

$$g_2 = 2/105, \tag{7}$$

$$v_2(y) = (675y^8 - 2940y^6 + 3570y^4 - 1020y^2 - 29)/201600, \tag{8}$$

$$g_3 = 4/17325. \tag{9}$$

These expansions were computed to high order and shown to converge for large scale structures, wave number  $|k| < 0.47$ .

## 2. Multi-mode models of channel dispersion

We construct models of dispersion in channels (1) based on the new proposed principle of matched centre manifolds. A multi-mode low-order model is sought which has the same centre manifold evolution as the original system—the agreement is to high order. This principle is rather like that employed in Padé approximation (and related schemes [1, Ch. 8]) where to improve the convergence of a Taylor series a rational function is constructed which has the same Taylor series to a specified order. Here we improve the resolution of a centre manifold model by constructing a multi-mode model with the same long term evolution, to some order in spatial derivatives.

Here we consider a two-component model. It eventuates that in effect one component is slow and the other is fast as in the zonal models of Chickwendu *et al.* [3, 4]. In this multi-mode model, we posit conservative exchange between the modes, and advection and diffusion within each mode, but no intermodal advection or diffusion. This is shown schematically in Figure 1, where the two modes are interpreted as two zones of different “widths” or “capacities”. A model system with these properties is

$$\frac{\partial \mathbf{u}}{\partial t} = A\mathbf{u} - B\frac{\partial \mathbf{u}}{\partial x} + D\frac{\partial^2 \mathbf{u}}{\partial x^2}, \quad (10)$$

where  $\mathbf{u} = (u_1, u_2)$ , and where

$$A = \begin{bmatrix} -a & a \\ b & -b \end{bmatrix}, \quad B = \begin{bmatrix} s_1 & 0 \\ 0 & s_2 \end{bmatrix}, \quad D = \begin{bmatrix} d_1 & 0 \\ 0 & d_2 \end{bmatrix}.$$

Observe that  $bu_1 + au_2$  is conserved; if  $u_1$  and  $u_2$  are considered to be “concentrations” in the zones, then the “width” of the zones is in the ratio of  $b : a$  (see Figure 1).

To determine the six constants of this model we match the long-term evolution of (1), as occurs on the centre manifold (3), with the long-term evolution of this model, as expressed on its centre manifold.

**2.1. The centre manifold of the model** As before, to construct the centre manifold we take derivatives with respect to  $x$  to be a small parameter. Dominantly, then

$$\frac{\partial \mathbf{u}}{\partial t} = A\mathbf{u},$$

and so the “concentrations” equilibrate between the zones with transients approximately like  $e^{-(a+b)t}$ . The centre manifold is then described in terms of the cross-zone weighted-average  $C = (bu_1 + au_2)/(a + b)$ . As usual [9], the centre manifold is constructed by assuming

$$\mathbf{u} = \mathcal{V}(C) \quad \text{such that} \quad \frac{\partial C}{\partial t} = \mathcal{G}(C),$$

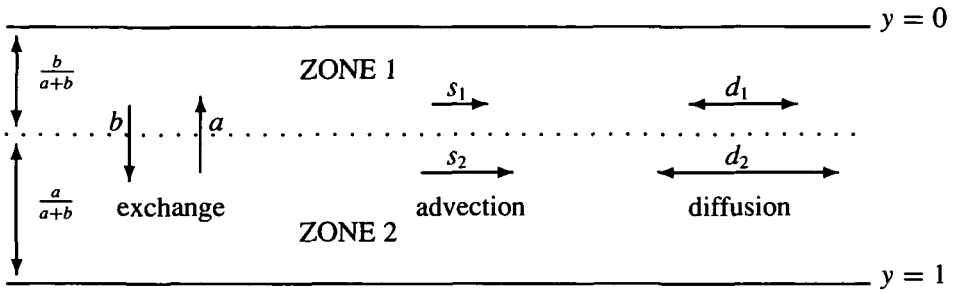


FIGURE 1. A schematic representation of the zonal model showing the three mechanisms of the channel-exchange, advection and diffusion.

and then seeking asymptotic expansions for  $\mathcal{V}$  and  $\mathcal{G}$  of the form

$$\mathcal{V} \sim \sum_{n=0}^{\infty} v_n \frac{\partial^n C}{\partial x^n} \quad \text{and} \quad \mathcal{G} \sim \sum_{n=1}^{\infty} g_n \frac{\partial^n C}{\partial x^n}.$$

Substituting these into the model equation (10), and collecting like longitudinal derivatives  $\partial^n C / \partial x^n$ , gives a hierarchy of equations

$$A v_n = \sum_{m=1}^n v_{n-m} g_m + B v_{n-1} - D v_{n-2}. \tag{11}$$

These together with amplitude conditions are easily solved to high order via the same form of the REDUCE program as used for the original system. For example, to second order, the evolution on the centre manifold is

$$\frac{\partial C}{\partial t} \sim -\bar{u} \frac{\partial C}{\partial x} + \bar{d} \frac{\partial^2 C}{\partial x^2},$$

where

$$\bar{u} = (b s_1 + a s_2) / (a + b) \tag{12}$$

is the appropriately weighted mean advection velocity, and the effective diffusivity is

$$\bar{d} = ab(s_1 - s_2)^2 / (a + b)^3 + (b d_1 + a d_2) / (a + b). \tag{13}$$

This effective diffusivity is the superposition of the weighted-mean diffusivity,  $(b d_1 + a d_2) / (a + b)$ , and the shear-dispersion term,  $ab(s_1 - s_2)^2 / (a + b)^3$ , which is proportional to the square of the velocity difference in the two zones. Using REDUCE we easily compute higher-order terms in the expansions.

**2.2. Matching for the advection model** The objective is to find a zonal model (10) whose evolution is “close” to the original system (1) of shear dispersion. Thus we must find good parameters to make the connection. A straightforward way, given that the evolution on both centre manifolds is known, is to assert that the long-term evolution on each manifold is the same to some order. As there are six degrees of freedom in the zonal model, those being the as yet undetermined parameters  $a$ ,  $b$ ,  $s_1$ ,  $s_2$ ,  $d_1$  and  $d_2$ , we determine an agreement up to sixth order in  $\partial/\partial x$ .

First, for comparison, we match both models for the case where there is no diffusion in the zonal model ( $d_1 = d_2 = 0$ ). This reduces the number of parameters by two and so we only seek agreement to fourth order.

Equating the coefficients of the first four derivatives of each evolution equation, namely (12) with (5), (13) with (7) and so on, gives four nonlinear equations in four unknowns. These equations have the solution

$$\begin{aligned} a &= \frac{4719}{812} - \frac{4719}{481516} \sqrt{7709} \approx 4.9511, \\ b &= \frac{4719}{812} + \frac{4719}{481516} \sqrt{7709} \approx 6.6721, \\ s_1 &= \frac{1887}{2030} + \frac{11}{2030} \sqrt{7709} \approx 1.4053, \\ s_2 &= \frac{1887}{2030} - \frac{11}{2030} \sqrt{7709} \approx 0.4539. \end{aligned}$$

As the parameters  $a$  and  $b$  are in essence the capacity of each zone, these results suggest that the fast zone should be thought of as nearly one and a half times as wide as the slow zone. Physically, we may imagine that the fast zone occupies the middle three-fifths of the channel, whereas the slow zone corresponds to the two outer fifths. However, this identification is refined in Section 3.4 when initial conditions are found.

Also, the second eigenvalue of the interaction matrix  $A$ , approximately the decay rate onto the centre manifold, is  $-(a + b)$ . Here this is  $-4719/406 \approx -11.62$ , which is comparable (perhaps fortuitously, but discussed later) to  $-\pi^2 \approx -9.8696$ , the decay rate of the first neglected symmetric mode of the original system (1), a difference of about 18%. Thus, not only is the long-term evolution nearly identical, but also the rate of approach to the shared long-term evolution is similar in both the model and the original.

**2.3. Matching with diffusion** Including the diffusion term in the zonal model makes the matching more difficult. Thus the equations are not solved analytically, but numerically. The solution obtained has  $a = 4.5669$  and  $b = 5.6569$  and values for  $s_1$ ,  $s_2$ ,  $d_1$  and  $d_2$  listed in Table 1. For comparison the coefficients found by Chickwendu [3] and the previous diffusionless model are also listed. The coefficients of the three models are very similar.

	Without diffusion	With diffusion	Chickwendu
$\eta_1$	0.5740	0.5533	0.5774
$\eta_2$	0.4260	0.4467	0.4226
$s_1$	1.4053	1.3829	1.3333
$s_2$	0.4539	0.5257	0.5447
$d_1$	-	$0.5043 \times 10^{-3}$	$0.7055 \times 10^{-3}$
$d_2$	-	$2.2426 \times 10^{-3}$	$1.4903 \times 10^{-3}$

TABLE 1. A comparison of the parameters for each of the three zonal models, where  $\eta_1 = b/(a + b)$  and  $\eta_2 = a/(a + b)$  as used by Chikwendu.

Note the presence of a pleasing physical feature in this zonal model. The low value of effective diffusivity in the fast zone,  $d_1$ , neatly corresponds to the limited shear of the fast flow in the centre of the channel, whereas the comparatively high value in the slow zone,  $d_2$ , matches the high shear found near the channel banks.

Lastly, the decay rate onto the centre manifold,  $-(a + b) = -10.2238$ , is again remarkably close to  $-\pi^2$ , a difference of about 3.6%. This closeness may be explained by noting that a centre manifold analysis is similar to that of a perturbed eigenproblem where here the derivative,  $\partial/\partial x$ , is the perturbing parameter. Typically, in a perturbed eigenproblem the different eigenvalues are analytic continuations of each other and are identifiable as different branches, or Riemann sheets, of the one analytic function [1, Section 7.5]. Thus the expansion for any one eigenvalue, here the neutral mode corresponding to the centre manifold, is affected by the other eigenvalues through their continuation in the complex plane. Hence it is plausible to expect that the exponentially decaying transients of the model, here dominantly  $\exp[-(a + b)t]$ , do correspond to physical dynamics in the original problem. However, due to the symmetry of the original problem about the channel centreline, the symmetric and antisymmetric Riemann sheets are completely decoupled. Hence the zonal model can only be affected by the symmetric channel modes.

**2.4. A comparison of our two zonal models** There are relatively minor differences between the widths and advection velocities for the models with and without diffusion: with diffusion the fast zone is a little “thicker” and slower while the slow zone is a little “smaller” and faster. For a further comparison between our two zonal models, we investigate how well the evolution on the centre manifold agrees between the two zonal models and the original system. Consider the asymptotic expansions for the evolution on the centre manifolds, of the form

$$G \sim \sum_{n=1}^{\infty} g_n \frac{\partial^n C}{\partial x^n}.$$

As discussed in Mercer and Roberts [7, Appendix], the validity of these expansions is related to the radius of convergence of the series. By using Roberts' generalisation of the Domb-Sykes formula

$$B_k^2 = \frac{g_{k+1}g_{k-1} - g_k^2}{g_k g_{k-2} - g_{k-1}^2},$$

the radius of convergence is given as

$$1/r_c = \lim_{k \rightarrow \infty} B_k.$$

Plotting  $B_k$  versus  $1/k$ , we extrapolate to find the radius of convergence,  $r_c$ , of each expansion. For the zonal model without diffusion, the radius of convergence is about 12.15. For the model with diffusion and the original system, both have a radius of convergence of about 11.8. (See Figure 2; note that the original system and the diffusive zonal model are almost indistinguishable.)

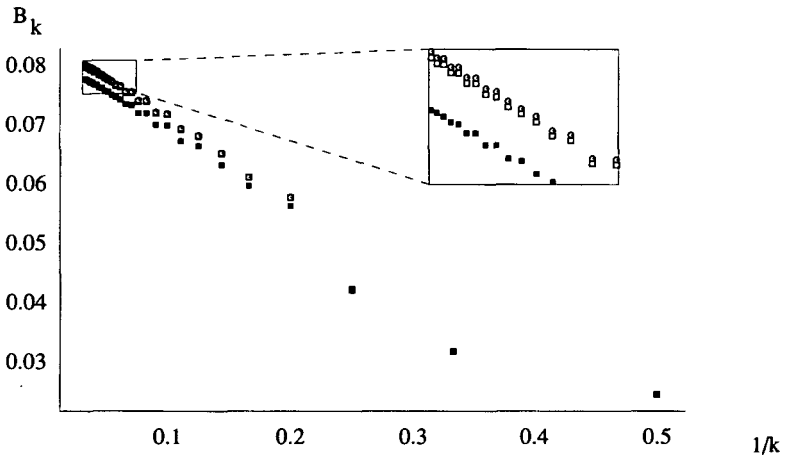


FIGURE 2. Generalised Domb-Sykes plot of the series of the  $B_k$ 's, for the original system and both zonal models, showing the close match of the evolution on the centre manifolds at high order. The original system is the dotted circle, the zonal model with diffusion is the empty squares, and the zonal model without diffusion is the filled squares.

This shows that by just matching evolutions at low order, important properties of the evolution on the centre manifold, such as convergence, are also closely matched at higher order: the model without diffusion is a good approximation; the model with diffusion an even closer approximation. However, this does not imply that the models will give identical behaviour inside their common radii of convergence. But it does imply that higher-order corrections to the zonal models are likely to be small because the high order behaviour is already closely matched to that of the centre manifold evolution of the original system.

### 3. Initial conditions

By centre manifold theory [2], for every trajectory starting near the centre manifold there is guaranteed to be a specific solution on the centre manifold which is approached exponentially quickly. Thus, for any initial distribution of contaminant,  $c^0$ , of the original system, there is an initial condition,  $C^0$ , for starting on the manifold so that the centre manifold solution approaches the exact solution exponentially quickly. Traditionally it has been assumed that  $C^0$  is just the cross-sectional average of the initial concentration. This is roughly correct, but is initially in error, and the errors persist for all time. Dynamically based arguments to derive the correct initial condition, given an original exact initial condition, were described by Roberts [10] for a general nonlinear system. For a linear system, such as the dynamics of shear dispersion, the derivation may be simplified as described by Watt and Roberts [15, Section 3]. It is the later formulation that is adopted here.

However, here we need to find an appropriate projection from the initial condition of the original system to the zonal model, as indicated by the dotted line labelled  $\zeta$  in Figure 3. This is found using the projection from the original system to the centre manifold,  $z$  on the figure, and that from the zonal model to the centre manifold,  $Z$  on the figure. Then  $\zeta$  is determined by requiring that the composition of the projection from the original system to the zonal and thence onto the centre manifold, is the same as that directly from the original system to the centre manifold; that is, we find  $\zeta$  so that  $Z \circ \zeta$  is the same, to some order, as  $z$ . To obtain the correct initial condition for the centre manifolds (solid arrows in Figure 3) we use the arguments and formulae developed by us [15, Section 3.1], and summarised below.

#### 3.1. Summary of the general linear analysis

Consider a general linear system

$$\dot{u} = \mathcal{A}u, \tag{14}$$

where  $\mathcal{A}$  is some particular linear operator (implicitly including boundary conditions if a differential operator), and the evolution on a low-dimensional invariant subspace  $u = \mathcal{V}c$ , where  $\mathcal{V}$  is a linear operator spanning the subspace. To be invariant under the evolution, this subspace must be spanned by a set of eigenvectors of  $\mathcal{A}$ . The evolution on the subspace may then be described by some low-dimensional evolution equation  $\dot{c} = \mathcal{G}c$

As previously argued [15, Section 3], there is a projection operator which will take any solution of the original system down onto a solution on the manifold, namely, that solution on the manifold which is approached exponentially. This operator  $(Z, \dots)$  may be expressed as

$$(Z, u(t)) = c(t), \tag{15}$$

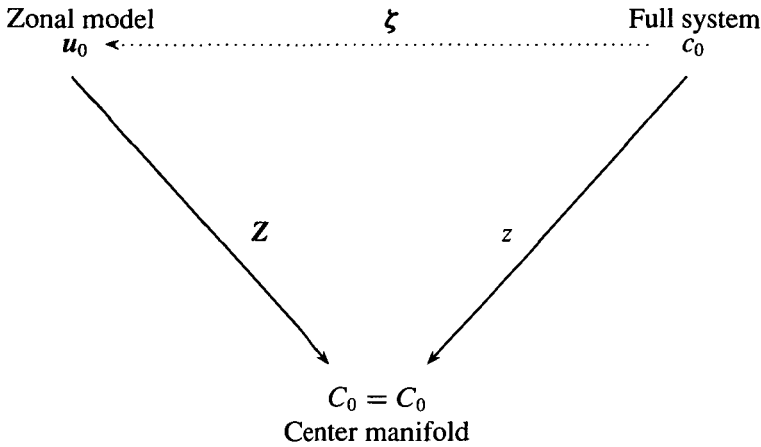


FIGURE 3. Diagram showing how the initial conditions of the zonal model are found given the initial condition of the original system, done by matching the initial condition on both centre manifolds.

for some inner product. For example, in the original system we use the inner product

$$(u, v) = \frac{1}{2} \int_{-1}^1 uv \, dy = \overline{uv}, \tag{16}$$

and in the zonal model, use

$$(u, v) = u^T v. \tag{17}$$

From [15], the projection  $Z$  is the solution of

$$\mathcal{A}^+ Z = Z \mathcal{G}^T \tag{18}$$

and the orthogonality equation

$$(Z, \mathcal{V}) = \mathcal{I}. \tag{19}$$

**3.2. Initial condition from the original system** For the centre manifold of the original system, (1), we identify

$$z \sim \sum_{n=0}^{\infty} z_n(y) \frac{\partial^n}{\partial x^n}, \quad \mathcal{G} \sim \sum_{n=1}^{\infty} g_n \frac{\partial^n}{\partial x^n}, \quad \mathcal{A} = \mathcal{L} + u(y) \frac{\partial}{\partial x},$$

where  $\mathcal{L} = \partial^2 / \partial y^2$  with boundary conditions of no flux across the channel boundaries.

Substituting these into (18) and collecting terms of the same order together yields

$$\mathcal{L}z_n = \sum_{m=1}^n z_{n-m}g_m + u(y)z_{n-1}.$$

Since  $\mathcal{L}$  is self-adjoint, this is in exactly the same form as (2.12) in [7], which was solved for the centre manifold of the original system. There are also the subsidiary conditions

$$\overline{z_0} = 1 \quad \text{and} \quad \sum_{m=0}^n \overline{z_{n-m}v_m} = 0,$$

as a consequence of the orthogonality constraint (19).

To the first few orders, the initial condition is

$$C^0 \sim \overline{z_0c^0} + z_1 \overline{\frac{\partial c^0}{\partial x}} + z_2 \overline{\frac{\partial^2 c^0}{\partial x^2}} + z_3 \overline{\frac{\partial^3 c^0}{\partial x^3}}, \tag{20}$$

where

$$\begin{aligned} z_0(y) &= 1, \\ z_1(y) &= -(15y^4 - 30y^2 + 7)/120, \\ z_2(y) &= (675y^8 - 2940y^6 + 3570y^4 - 1020y^2 - 413)/201600, \\ z_3(y) &= -(675y^{12} - 4642y^{10} + 10725y^8 - 8316y^6)/17740800 \\ &\quad + (10705695y^4 - 23060310y^2 + 4076777)/24216192000. \end{aligned}$$

as recorded by Mercer and Roberts [7]. Higher orders were also computed in order to perform the matching.

**3.3. Initial condition from the zonal model** For the zonal model we identify

$$\mathbf{Z} \sim \sum_{n=0}^{\infty} \mathbf{Z}_n \frac{\partial^n}{\partial x^n}, \quad \mathcal{G} \sim \sum_{n=1}^{\infty} g_n \frac{\partial^n}{\partial x^n}, \quad \mathcal{A} = A - B \frac{\partial}{\partial x} + D \frac{\partial^2}{\partial x^2}.$$

Substituting these into (18) and collecting terms of the same order together, yields

$$A^T \mathbf{Z}_n = \sum_{m=1}^n \mathbf{Z}_{n-m}g_m + B^T \mathbf{Z}_{n-1} - D^T \mathbf{Z}_{n-2}.$$

As can be seen, this is in the same form as (11). The differences are that the matrices are transposed and that now an orthogonality constraint,

$$\mathbf{Z}_0^T \mathbf{v}_0 = 1 \quad \text{and} \quad \sum_{m=0}^n \mathbf{Z}_{n-m}^T \mathbf{v}_m = 0,$$

needs to be satisfied.

Solving this hierarchy of equations to the first few orders, we deduce that the initial condition for the centre manifold of the zonal model is approximately

$$C^0 \sim \mathbf{Z}_0^T \mathbf{u}^0 + \mathbf{Z}_1^T \frac{\partial \mathbf{u}^0}{\partial x} + \mathbf{Z}_2^T \frac{\partial^2 \mathbf{u}^0}{\partial x^2} + \mathbf{Z}^T \frac{\partial^3 \mathbf{u}^0}{\partial x^3}, \tag{21}$$

where

$$\begin{aligned} \mathbf{Z}_0 &= \frac{1}{a+b} \begin{bmatrix} b \\ a \end{bmatrix}, \\ \mathbf{Z}_1 &= \frac{ab(s_1 - s_2)}{(a+b)^3} \begin{bmatrix} -1 \\ 1 \end{bmatrix}, \\ \mathbf{Z}_2 &= \frac{ab(s_1 - s_2)^2}{(a+b)^5} \begin{bmatrix} a - 2b \\ b - 2a \end{bmatrix} + \frac{ab(d_1 - d_2)}{(a+b)^3} \begin{bmatrix} 1 \\ -1 \end{bmatrix}, \\ \mathbf{Z}_3 &= \frac{ab(s_1 - s_2)^3}{(a+b)^7} \begin{bmatrix} -a^2 + 6ab - 3b^2 \\ 3a^2 - 6ab + b^2 \end{bmatrix} + \frac{ab(s_1 - s_2)(d_1 - d_2)}{(a+b)^5} \begin{bmatrix} a - 2b \\ 2a - b \end{bmatrix}. \end{aligned}$$

Higher orders were also calculated to be used for the matching.

**3.4. Matching without diffusion** We now find the  $\mathbf{u}^0$  for which the zonal model matches a given  $c^0$  by equating the expressions (20) and (21) for the two initial conditions found on the centre manifold.

Suppose  $\mathbf{u}^0$  is given by a projection of the form

$$\mathbf{u}^0 = \overline{\zeta_0(y)c^0} + \overline{\zeta_1(y) \frac{\partial c^0}{\partial x}}, \tag{22}$$

where the as yet unknown  $2 \times 1$  matrices  $\zeta_0$  and  $\zeta_1$  are to be determined by matching. Now the initial condition on the centre manifold direct from the original system is (20), whereas that for the centre manifold of the zonal model after the as yet unknown projection (22) from the original system onto the model is

$$\begin{aligned} C^0 &= \overline{\mathbf{Z}_0^T \zeta_0 c^0} + \overline{\mathbf{Z}_0^T \zeta_1 \frac{\partial c^0}{\partial x}} \\ &\quad + \overline{\mathbf{Z}_1^T \zeta_0 \frac{\partial c^0}{\partial x}} + \overline{\mathbf{Z}_1^T \zeta_1 \frac{\partial^2 c^0}{\partial x^2}} \\ &\quad + \overline{\mathbf{Z}_2^T \zeta_0 \frac{\partial^2 c^0}{\partial x^2}} + \overline{\mathbf{Z}_2^T \zeta_1 \frac{\partial^3 c^0}{\partial x^3}} + \dots \end{aligned}$$

These two expressions for  $C^0$  must be equal for all initial distributions  $c^0$ , so we equate coefficients of  $c^0$  and its derivatives. Equating the four integrands up to  $3^{rd}$  order, we get four scalar equations in the unknown  $\zeta_0$  and  $\zeta_1$ :

$$\begin{aligned} z_0(y) &= \mathbf{Z}_0^T \zeta_0, \\ z_1(y) &= \mathbf{Z}_0^T \zeta_1 + \mathbf{Z}_1^T \zeta_0, \\ z_2(y) &= \mathbf{Z}_1^T \zeta_1 + \mathbf{Z}_2^T \zeta_0, \\ z_3(y) &= \mathbf{Z}_2^T \zeta_1 + \mathbf{Z}_3^T \zeta_0. \end{aligned}$$

Solving these linear equations gives

$$\begin{aligned} \zeta_0 &= \begin{bmatrix} 1.2580 \\ 0.6524 \end{bmatrix} z_0 + \begin{bmatrix} 21.28 \\ -28.68 \end{bmatrix} z_1 + \begin{bmatrix} -157.40 \\ 212.0 \end{bmatrix} z_2 + \begin{bmatrix} 6493 \\ -17498 \end{bmatrix} z_3, \\ \zeta_1 &= \begin{bmatrix} -0.03588 \\ 0.06332 \end{bmatrix} z_0 + \begin{bmatrix} 1.7420 \\ 2.348 \end{bmatrix} z_1 + \begin{bmatrix} -26.76 \\ 18.708 \end{bmatrix} z_2 + \begin{bmatrix} 452.8 \\ 822.4 \end{bmatrix} z_3. \end{aligned}$$

These functions are shown graphically in Figure 4. Observe from Figure 4(a) that any contaminant released near the channel centre is assigned to the fast zone mode, whereas any released near the banks is assigned to the slow zone mode. However, there is no sharp boundary between the physical zones; the transition is smooth. Also observe that the corrections  $\zeta_1$ , shown in Figure 4(b), are about 1% of  $\zeta_0$ , hence only steep gradients in the initial concentration alter the leading order in the initial condition (22).

**3.5. Matching with diffusion** Following the same method as in the previous subsection, we find  $\mathbf{u}^0$  given  $c^0$ , except now we suppose  $\mathbf{u}^0$  is of the form

$$\mathbf{u}^0 = \overline{\zeta_0(y)c^0} + \zeta_1(y) \frac{\partial c^0}{\partial x} + \zeta_2(y) \frac{\partial^2 c^0}{\partial x^2}.$$

Equating the integrands up to 5<sup>th</sup> order, we get six equations in the unknown  $\zeta_n$  functions:

$$\begin{aligned} z_0(y) &= \mathbf{Z}_0^T \zeta_0, \\ z_1(y) &= \mathbf{Z}_0^T \zeta_1 + \mathbf{Z}_1^T \zeta_0, \\ z_2(y) &= \mathbf{Z}_0^T \zeta_2 + \mathbf{Z}_1^T \zeta_1 + \mathbf{Z}_2^T \zeta_0, \\ z_3(y) &= \mathbf{Z}_1^T \zeta_2 + \mathbf{Z}_2^T \zeta_1 + \mathbf{Z}_3^T \zeta_0, \\ z_4(y) &= \mathbf{Z}_2^T \zeta_2 + \mathbf{Z}_3^T \zeta_1 + \mathbf{Z}_4^T \zeta_0, \\ z_5(y) &= \mathbf{Z}_3^T \zeta_2 + \mathbf{Z}_4^T \zeta_1 + \mathbf{Z}_5^T \zeta_0. \end{aligned}$$

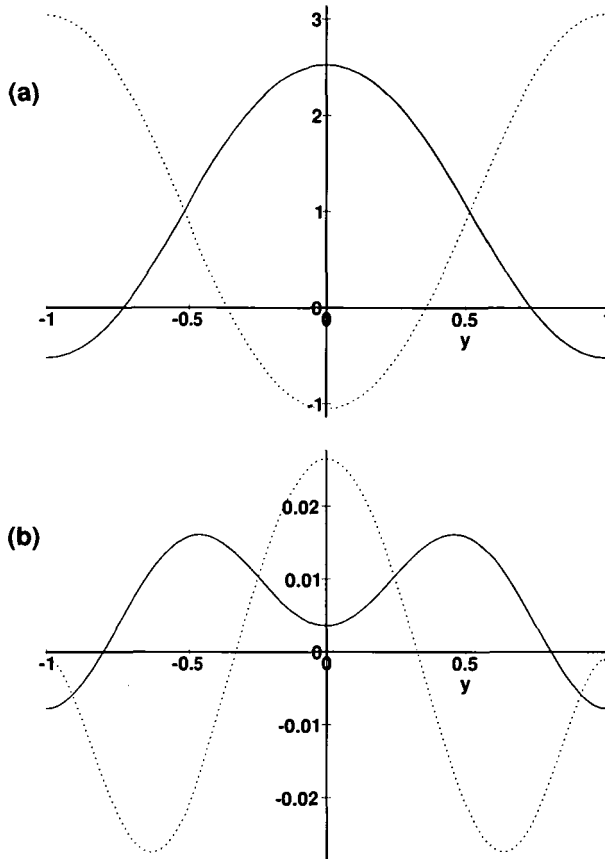


FIGURE 4. Graphs of the initial condition functions as a function of  $y$  for the zonal model without diffusion: (a)  $\zeta_0$ ; (b)  $\zeta_1$ . The solid line (—) is for the fast zone,  $\zeta_{n1}$ , and the dotted line (⋯⋯) is for the slow zone,  $\zeta_{n2}$ .

Solving these linear equations, we find

$$\begin{aligned} \zeta_0(y) &= \begin{bmatrix} 1.4928 \\ 0.4144 \end{bmatrix} z_0 + \begin{bmatrix} 21.56 \\ -26.70 \end{bmatrix} z_1 + \begin{bmatrix} -0.3796 \\ 0.4702 \end{bmatrix} z_2 \\ &\quad + \begin{bmatrix} -25636 \\ 31756 \end{bmatrix} z_3 + \begin{bmatrix} 156000 \\ -96616 \end{bmatrix} z_4 + \begin{bmatrix} -7121926 \\ 8821738 \end{bmatrix} z_5, \\ \zeta_1(y) &= \begin{bmatrix} -0.06074 \\ 0.11436 \end{bmatrix} z_0 + \begin{bmatrix} 1.7638 \\ 2.292 \end{bmatrix} z_1 + \begin{bmatrix} 21.50 \\ -26.66 \end{bmatrix} z_2 \\ &\quad + \begin{bmatrix} -763.6 \\ -1716.8 \end{bmatrix} z_3 + \begin{bmatrix} 16194 \\ 3856 \end{bmatrix} z_4 + \begin{bmatrix} -174428 \\ -523658 \end{bmatrix} z_5, \end{aligned}$$

$$\zeta_2(y) = \begin{bmatrix} -0.0010058 \\ -0.002914 \end{bmatrix} z_0 + \begin{bmatrix} 0.00009333 \\ -0.00010574 \end{bmatrix} z_1 + \begin{bmatrix} 1.7612 \\ 2.290 \end{bmatrix} z_2 \\ + \begin{bmatrix} -61.08 \\ 90.70 \end{bmatrix} z_3 + \begin{bmatrix} 649.6 \\ 303.2 \end{bmatrix} z_4 + \begin{bmatrix} -9646 \\ 20038 \end{bmatrix} z_5.$$

These functions are shown graphically in Figure 5. As in Figure 4(a), most of the contribution to the initial condition of the fast zone comes from the middle of the channel, the location of the fast zone, and most of the initial condition of the slow zone comes from near the banks, the location of the slow zone.

**3.6. Comparative results** Using these initial conditions for both zonal models, we compare the original system with the approximate models *via* some numerical simulations. As well as comparing the two zonal models with the original system (1), we also include predictions for the centre manifold model (2) with initial condition (20).

The numerical simulations employed simple finite difference schemes for each model and the original system. The channel is long enough so that neither the inlet nor the outlet had any influence on the contaminant field.

The initial contaminant field chosen for the comparison was a mid-channel release of the form

$$c^0(x, y) = \exp[-(2x)^{12} - (4y)^{12}],$$

which approximates a box of length 1 and width 0.5 at the centre of the channel. The property chosen to base the comparison on was the average concentration across the channel, as a function of downstream position. This is shown in Figure 6 at time  $t = 0.1$ .

From this figure, it can be seen that both zonal models are very good approximations for this small time, indeed they are both nearly indistinguishable from the exact solution, with the zonal model with diffusion better than the model without diffusion (see inset). Importantly, the matching process used to guarantee a long-term agreement between model and original, here also produces excellent short-term predictions.

Observe that all three models predict a concentration which is negative in a very small region at the “tail” of the profile, near  $x \approx -0.5$ . This is due to the corrections of the initial conditions and the fact the contaminant is conserved. As shown in [15] such negative concentrations are a necessary condition for long-term agreement between model and original system.

We also ran the model to obtain solutions for time  $t = 1$  to show a little of the long-term agreement between the dynamics. In Figure 7, the errors in the zonal models are shown to be typically less than  $10^{-4}$ , with the higher-order diffusion model being the better. The centre manifold model has errors which are two orders of magnitude larger – still small because correct initial conditions ensure a long-term agreement, but not as good as the zonal models.

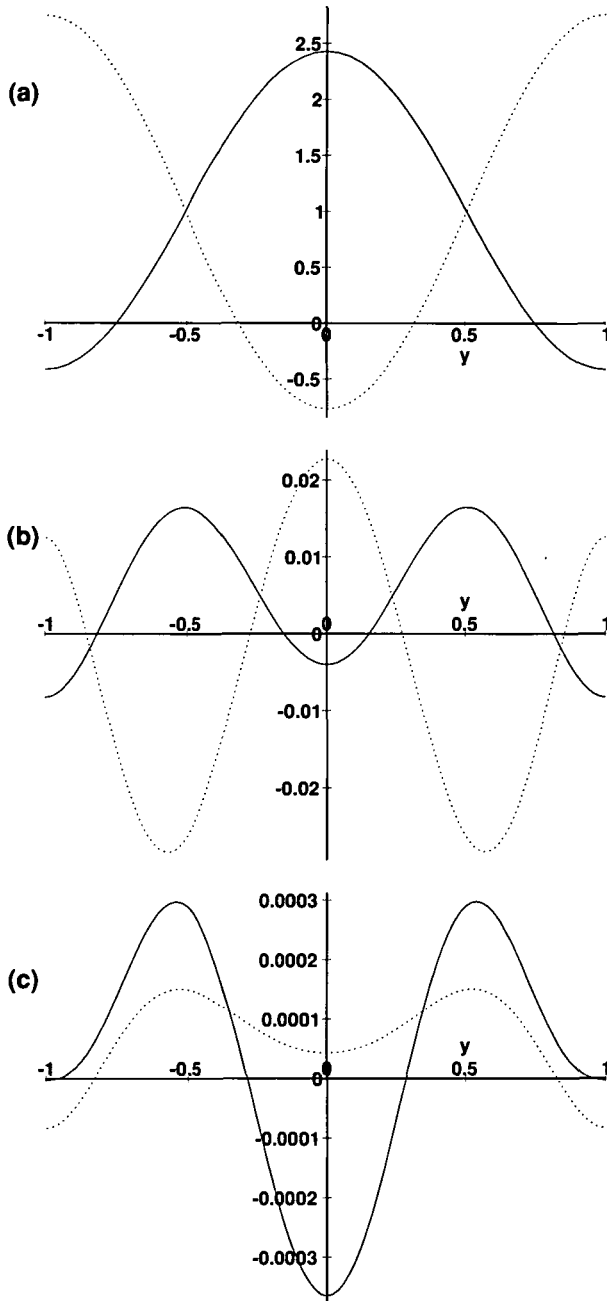


FIGURE 5. Graphs of the initial condition functions as a function of  $y$  for the zonal model with diffusion: (a)  $\zeta_0$ ; (b)  $\zeta_1$ ; (c)  $\zeta_2$ . The solid line (—) is for the fast zone,  $\zeta_{n1}$ , and the dotted line (·····) is for the slow zone,  $\zeta_{n2}$ .

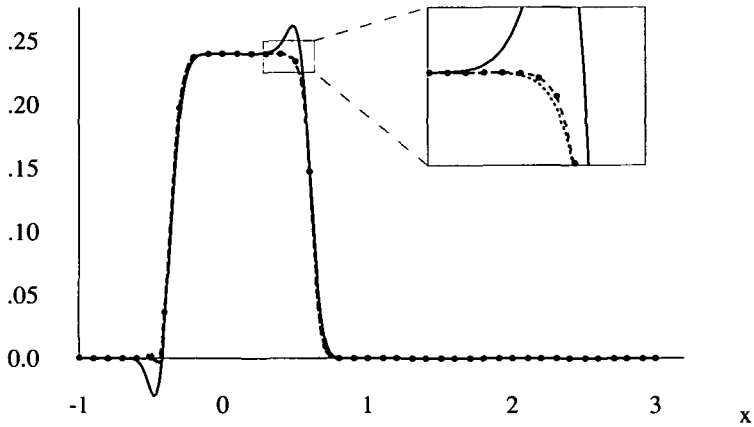


FIGURE 6. Comparison of the mean concentration of each model at time  $t = 0.1$  where: the centre manifold model (2) is the solid line (—); the zonal model without diffusion is the short-dashed line (- - - -); the zonal model with diffusion is the dashed line (- - -); and the original system (1) is shown by the discs (.). Each model simulation started from the initial conditions determined in this section.

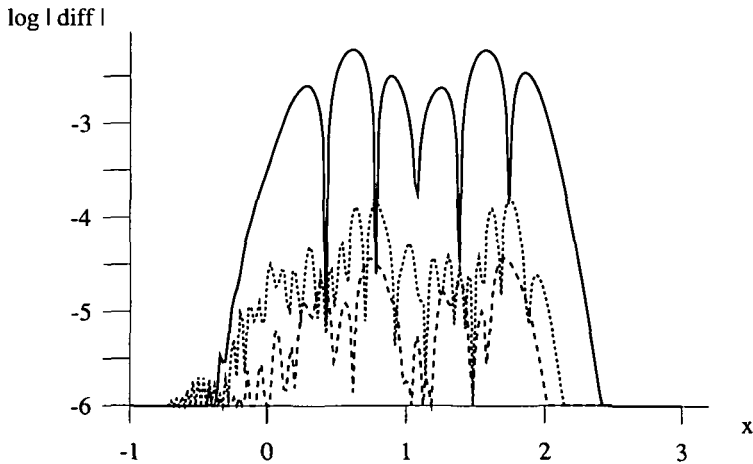


FIGURE 7. The log (to base 10) of the difference between a model and the original system at time  $t = 1$ : the centre manifold model of Section 1.1 is the solid line (—); the zonal model without diffusion of Section 2.2 is the small-dashed line (- - -); and the zonal model with diffusion of Section 2.3 is the dashed line (- - -). Each model simulation started from the initial conditions determined in this section.

#### 4. Boundary conditions

The zonal models (10) are partial differential equations in space and time. Hence spatial boundary conditions need to be specified before the equations are solved. We find boundary conditions via adaptations of the method developed by Roberts [11] for centre manifold models.

**4.1. Inlet boundary conditions** First the inlet boundary condition of the zonal model is found as a function of the inlet boundary condition of the original system. As explained in [11], finding the appropriate boundary condition on the centre manifold is similar to that of finding the initial condition on the centre manifold, except that here the governing equations are taken to describe the evolution in space given slow time variations. The “initial” condition of the spatial evolution is equivalent to the inlet boundary condition of the time evolution.

The equations for both the original system and the zonal model (without diffusion) are rewritten respectively as

$$\begin{aligned}\mathcal{L}c &= u(y)\frac{\partial c}{\partial x} + \frac{\partial c}{\partial t}, \\ Au &= B\frac{\partial u}{\partial x} + \frac{\partial u}{\partial t},\end{aligned}$$

which are (1) and (10) (without the diffusion term), except that here the “advection” coefficients,  $u(y)$  and  $B$  respectively, multiply what we now consider as the “time-like” derivative.

We perform the same analysis as in Sections 1 and 2, to get the approximation to the centre manifolds of the spatial evolution

$$\begin{aligned}c &\sim w_0C + w_1\frac{\partial C}{\partial t} + w_2\frac{\partial^2 C}{\partial t^2} + \dots, \\ u &\sim w_0C + w_1\frac{\partial C}{\partial t} + w_2\frac{\partial^2 C}{\partial t^2} + \dots,\end{aligned}$$

where

$$\begin{aligned}w_0(y) &= 1, \\ w_1(y) &= (15y^4 - 30y^2 + 7)/120, \\ w_2(y) &= (675y^8 - 2940y^6 + 3090y^4 - 60y^2 - 253)/201600,\end{aligned}$$

and

$$\mathbf{w}_0 = \begin{bmatrix} 1 \\ 1 \end{bmatrix},$$

$$w_1 = \frac{s_1 - s_2}{(a + b)(as_2 + bs_1)} \begin{bmatrix} a \\ -b \end{bmatrix},$$

$$w_2 = \frac{(s_1 - s_2)^2(a^2s_2 - b^2s_1)}{(a + b)^2(as_2 + bs_1)^3} \begin{bmatrix} a \\ -b \end{bmatrix},$$

where the evolution on the centre manifold of the original system is

$$\frac{\partial C}{\partial x} \sim -\frac{\partial C}{\partial t} + \frac{2}{105} \frac{\partial^2 C}{\partial t^2} + \dots, \tag{23}$$

and the evolution on the centre manifold of the zonal model is

$$\frac{\partial C}{\partial x} \sim -\bar{u}' \frac{\partial C}{\partial t} + \bar{d}' \frac{\partial^2 C}{\partial t^2} + \dots, \tag{24}$$

where

$$\bar{u}' = (a + b)/(as_2 + bs_1) \quad \text{and} \quad \bar{d}' = (ab(s_1 - s_2)^2)/((as_2 + bs_1)^3).$$

By equating the coefficients of the first four derivatives in the evolution equation (23) with the first four coefficients in (24), we find that the parameters of the zonal model  $a$ ,  $b$ ,  $s_1$  and  $s_2$  are exactly the same as those determined in Section 2.2. As the temporal and spatial evolution equations are closely related, the reversion of each other, it would be expected that the parameters will be the same. Thus, this is a useful confirmation that the derived evolution equations are correct, but does not give any new information.

By following the method outlined in Section 3, we find the inlet boundary condition of the centre manifold corresponding to the inlet boundary condition of the original system and the zonal model. The inner product used is a weighted average with respect to the velocity,  $u(y)$  and  $B$  respectively, that is,

$$\langle \alpha, \beta \rangle = \frac{1}{2} \int_{-1}^1 u(y)\alpha(y)\beta(y) dy = \overline{u\alpha\beta},$$

is the inner product for the original system, and

$$\langle \alpha, \beta \rangle = \alpha^T B \beta,$$

is the inner product for the zonal model. The inlet condition for the centre manifold of the original system is found to be

$$C(0, t) \sim \overline{up_0c(0, t)} + \overline{up_1 \frac{\partial c}{\partial t}(0, t)} + \overline{up_2 \frac{\partial^2 c}{\partial t^2}(0, t)} + \dots, \tag{25}$$

where

$$\begin{aligned}
 p_0(y) &= 1, \\
 p_1(y) &= (105y^4 - 210y^2 + 17)/840, \\
 p_2(y) &= (51975y^8 - 226380y^6 + 164010y^4 + 143220y^2 - 39001)/15523200.
 \end{aligned}$$

The inlet condition of the centre manifold corresponding to the zonal model is

$$C(0, t) \sim P_0^T B u(0, t) + P_1^T B \frac{\partial u}{\partial t}(0, t) + P_2^T B \frac{\partial^2 u}{\partial t^2}(0, t) + \dots, \tag{26}$$

where

$$\begin{aligned}
 P_0 &= \frac{1}{as_2 + bs_1} \begin{bmatrix} b \\ a \end{bmatrix}, \\
 P_1 &= \frac{ab(s_1 - s_2)}{(a + b)(as_2 + bs_1)^3} \begin{bmatrix} as_2 - 2as_1 - bs_1 \\ as_2 + 2bs_2 - bs_1 \end{bmatrix}, \\
 P_2 &= \frac{3ab(s_1 - s_2)^2}{(a + b)(as_2 + bs_1)^5} \begin{bmatrix} bs_2(as_2 - 2as_1 - bs_1) \\ as_1(bs_1 - 2bs_2 - as_2) \end{bmatrix} + \frac{ab(s_1 - s_2)^2}{(a + b)(as_2 + bs_1)^3} \begin{bmatrix} 1 \\ 1 \end{bmatrix}.
 \end{aligned}$$

Now we can proceed to find the inlet condition for the zonal model. Assume  $u(0, t)$  is given from  $c(0, t)$  by an expression of the form

$$u(0, t) = \overline{u(y)\zeta_0(y)c(0, t)} + \overline{u(y)\zeta_1(y)\frac{\partial c}{\partial t}(0, t)}. \tag{27}$$

Compare (25) with the results of the appropriate transform, (27) followed by (26) and require that the coefficients of  $c(0, t)$  and its derivatives are equal to obtain

$$\begin{aligned}
 p_0(y) &= P_0^T B \zeta_0, \\
 p_1(y) &= P_0^T B \zeta_1 + P_1^T B \zeta_0, \\
 p_2(y) &= P_1^T B \zeta_1 + P_2^T B \zeta_0, \\
 p_3(y) &= P_2^T B \zeta_1 + P_3^T B \zeta_0.
 \end{aligned}$$

The solution to these linear equations is

$$\begin{aligned}
 \zeta_0(y) &= \begin{bmatrix} 1.9242 \\ -2.858 \end{bmatrix} p_0 + \begin{bmatrix} -20.40 \\ 85.14 \end{bmatrix} p_1 + \begin{bmatrix} -1003.6 \\ 4188 \end{bmatrix} p_2 + \begin{bmatrix} -14490 \\ 60466 \end{bmatrix} p_3, \\
 \zeta_1(y) &= \begin{bmatrix} 0.010256 \\ -0.2642 \end{bmatrix} p_0 + \begin{bmatrix} 1.6112 \\ 5.418 \end{bmatrix} p_1 + \begin{bmatrix} 31.02 \\ 213.4 \end{bmatrix} p_2 + \begin{bmatrix} 229.2 \\ 3994 \end{bmatrix} p_3.
 \end{aligned}$$

These functions are shown graphically in Figure 8. Note that the integral (27) has been weighted by the advection velocity  $u(y)$ . Thus they apply directly to the cross-channel

distribution of the flux of contaminant at the inlet. The dominant contribution to the fast zone is from the centre region of the channel, the dominant positive contribution to the slow zone is from the sides of the channel. Note the negative contribution to the slow zone from a mid-channel injection: a negative concentration travelling slowly in the slow zone of the model, in effect, increases the speed and reduces dispersion of the model's predictions—as appropriate for an injection into the fast flow and little shear of the channel centre.

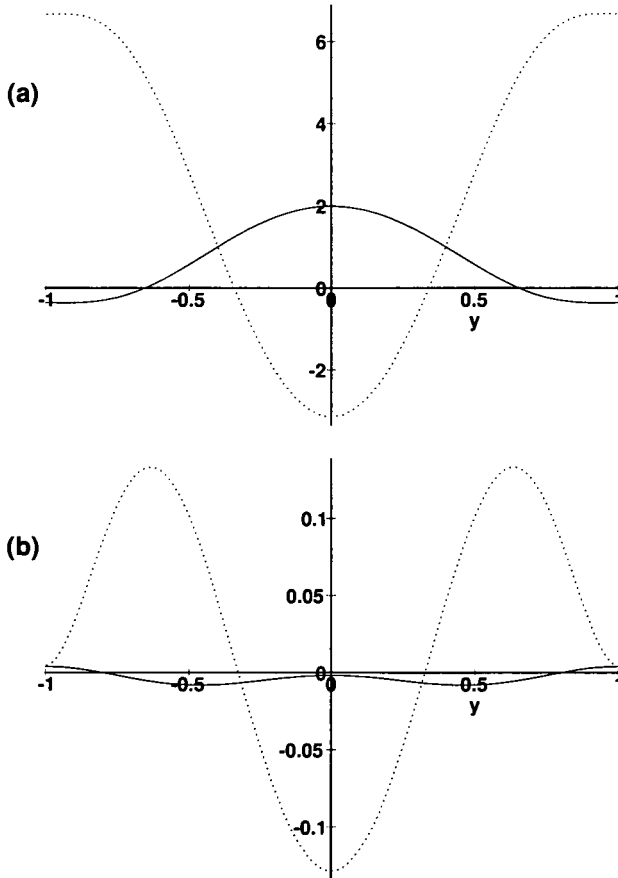


FIGURE 8. Graphs of the boundary condition functions as a function of  $y$  for the zonal model without diffusion: (a)  $\zeta_0$ ; (b)  $\zeta_1$ . The solid line (—) is for the fast zone,  $\zeta_{n1}$ , and the dotted line ( $\cdots$ ) is for the slow zone,  $\zeta_{n2}$ .

These two prescribed-inlet boundary conditions give enough boundary conditions for the advection model to form a well-posed model.

The corrections to the boundary conditions are required so that the approximate

models and original system are asymptotically equal, as described in [11]. However, if the boundary conditions of the original system are independent of time, the boundary conditions of the zonal models are just a weighted average of the inlet concentrations.

**4.2. Physical boundary conditions** For the model with diffusion, given the inlet boundary conditions of the previous section (or a modification thereof), a further two boundary conditions are needed to form a well-posed model.

Consider the zonal model

$$\frac{\partial \mathbf{u}}{\partial t} = A\mathbf{u} - B\frac{\partial \mathbf{u}}{\partial x} + D\frac{\partial^2 \mathbf{u}}{\partial x^2}.$$

Converting the zonal model (10) to a system of first-order partial differential equations with space- as the time-like variable gives

$$\frac{\partial \mathbf{u}}{\partial x} = \mathbf{v}, \quad (28)$$

$$D\frac{\partial \mathbf{v}}{\partial x} = \frac{\partial \mathbf{u}}{\partial t} - A\mathbf{u} + B\mathbf{v}. \quad (29)$$

Substituting

$$\begin{bmatrix} \mathbf{u} \\ \mathbf{v} \end{bmatrix} (= \mathbf{U}) \sim \mathbf{k}e^{\lambda x}$$

into (28–29) leads to a perturbed eigenvalue problem if the time derivative,  $\partial/\partial t$ , is assumed to be a “small” perturbation. The eigenvalues of this system are  $\lambda_1 \approx 2745$ ,  $\lambda_2 \approx 244$ ,  $\lambda_3 \approx 0$  and  $\lambda_4 \approx -13$ .

- The approximate zero eigenvalue corresponds to the slow evolution in the interior of the domain.
- Near the inlet, there will be transients behaving like  $e^{-13x}$ . These are acceptable as they correspond to the not-so-fast relaxation from the two inlet conditions (27) to the slowly-varying interior dynamics.
- However, near the exit, there are two rapid exponential transients arising from modes corresponding to the large positive eigenvalues  $\lambda_1$  and  $\lambda_2$ . These modes must not be present and boundary conditions are here found to eliminate them.

Suppose the system (28–29) has eigensolutions  $\{\lambda_k; \mathbf{z}_k; \mathbf{u}_k\}$  where  $\lambda_k$  is the eigenvalue,  $\mathbf{z}_k$  is the left eigenvector corresponding to  $\lambda_k$ ,  $\mathbf{u}_k$  is the right eigenvector corresponding to  $\lambda_k$ , and  $\mathbf{z}_i^T \mathbf{u}_j = \delta_{ij}$ . Now the solution at the exit,  $x = L$ , is

$$\mathbf{U}(L, t) = \sum_{i=1}^4 \alpha_i(t) \mathbf{u}_i,$$

where  $\alpha_i(t) = z_i^T U(L, t)$ . To eliminate the modes corresponding to  $\lambda_1$  and  $\lambda_2$  at the exit, we thus require

$$\begin{bmatrix} z_1^T \\ z_2^T \end{bmatrix} U = \mathbf{0} \quad \text{at } x = L.$$

This gives two boundary conditions in the four unknowns.

At leading order

$$\frac{\partial u}{\partial x} \sim \begin{bmatrix} -3.2862 & 3.2862 \\ 10.177 & -10.177 \end{bmatrix} u,$$

which asserts that any concentration difference between the fast and slow zone must correspond to a specific spatial gradient in the zones. These allowed spatial gradients correspond to the relatively slow dynamics, roughly  $e^{0x}$  and  $e^{-13x}$ , in the model which have some physical basis.

### 5. Conclusion

We have combined some of the best features of two different approaches to modelling shear dispersion into a single approach. The first approach is that of using centre manifold theory to derive a generalised Taylor description of dispersion. The advantage of this particular approach is that it is a straightforward mechanistic process to find high-order approximations. Its disadvantage is its limited spatio-temporal resolution. The second approach is to derive a zonal model of dispersion. Here we developed a two-zone model, the two zones corresponding to a fast zone and a slow zone. Previously [3], the coefficients of such a model have been obtained by heuristic arguments. Here centre manifold techniques are used to form a description of the long-term behaviour of this model, then by matching it is possible to find the various parameters of the interaction, advection and diffusion in the zonal model. In essence, this is the same principle as that employed in constructing Padé approximations of a power series.

That the principle can work is shown by the excellent agreement exhibited in Section 3.6 between the predictions of the zonal model and the solutions of the original system. Although we have not been able to quantify the spatial resolution of the zonal models (as has been done for other dispersion models [7, 15, 8]), nonetheless, Figure 6 indicates that the resolution is significantly improved.

As noted in Section 2, we reasonably expect the exponential transients of such a zonal system to approximately model actual physical dynamics; this is because physical transients are a continuation of the centre manifold expansion through the complex plane by being different branches of the one analytic function. However, in this problem the Riemann sheets of the symmetric and asymmetric modes are entirely disjoint—due to symmetry of the problem there is no interaction between the two

types of modes. Thus a zonal model constructed by matching centre manifolds can never “know” about dynamics of the asymmetric modes, and is thus deficient in the asymmetric dynamics. To construct a zonal model that resolves some asymmetric dynamics, perhaps we would need to introduce some asymmetry in order to couple the symmetric and asymmetric modes.

By using asymptotically correct initial conditions, we compared the various models in Section 3.6. This demonstrated the close agreement of the zonal models with the original system at small time. By changing the view of the evolution from temporal to spatial [11], we followed the same matching procedure to obtain inlet conditions of the zonal model given the inlet boundary conditions of the original system. Outlet boundary conditions were obtained, as in [11], by requiring that there be no unphysically rapid transients at the outlet.

This new method of matching centre manifolds allows us to systematically derive low-dimensional models, *complete* with initial and boundary conditions. Furthermore, the derivation, based on centre manifold analysis, is significantly simpler than the comparable invariant manifold analysis [15].

There are a few ways in which this model could be extended. The first is to find the inlet condition of the zonal model with diffusion. It was not done here as it is more complicated, and should not give any qualitatively different results. A second is to include more general interactions such as interzonal diffusion into the zonal model. This is possible as all we would do is to calculate the evolution on each centre manifold to another couple of orders. A final extension would be to introduce a third zone (as was briefly discussed in [4]), but this would not by itself introduce asymmetry into the zonal model—a new idea is needed to overcome this deficit.

## References

- [1] C. M. Bender and S. A. Orszag, *Advanced mathematical methods for scientists and engineers* (McGraw-Hill, New York, 1978).
- [2] J. Carr, *Applications of centre manifold theory*, Applied Mathematical Sciences, **35**, (Springer-Verlag, New York, 1981).
- [3] S. C. Chickwendu, “Application of a slow-zone model to contaminant dispersion in laminar shear flows”, *Intl. J. Engng. Sci.* **24** (1986) 1031–1044.
- [4] S. C. Chickwendu and G. U. Ojiakor, “Slow-zone model for longitudinal dispersion in two-dimensional shear flows”, *J. Fluid Mech.* **152** (1985) 15–38.
- [5] P. H. Coullet and E. A. Spiegel, “Amplitude equations for systems with competing instabilities”, *SIAM J. Appl. Math.* **43** (1983) 776–821.
- [6] W. N. Gill and R. Sankarasubramanian, “Exact analysis of unsteady convective diffusion”, *Proc. Roy. Soc. Lond. A* **316** (1970) 341–350.
- [7] G. N. Mercer and A. J. Roberts, “A centre manifold description of contaminant dispersion in channels with varying flow properties”, *SIAM J. Appl. Math.* **50** (1990) 1547–1565.

- [8] G. N. Mercer and A. J. Roberts, "A complete model of shear dispersion in pipes", *Japan J. Indust. Appl. Math.* **11** (1994) 499–521.
- [9] A. J. Roberts, "Simple examples of the derivation of amplitude equations for systems of equations possessing bifurcations", *J. Austral. Math. Soc. Ser. B* (1985) 48–65.
- [10] A. J. Roberts, "Appropriate initial conditions for asymptotic descriptions of the long term evolution of dynamical systems", *J. Austral. Math. Soc. Ser. B* **31** (1989) 48–75.
- [11] A. J. Roberts, "Boundary conditions for approximate differential equations", *J. Austral. Math. Soc. Ser. B* **34** (1992) 54–80.
- [12] A. J. Roberts, "Planform evolution in convection—an embedded centre manifold", *J. Austral. Math. Soc. Ser. B* **34** (1992) 174–198.
- [13] R. Smith, "Diffusion in shear flows made easy: the Taylor limit", *J Fluid Mech* **175** (1987) 201–214.
- [14] G. I. Taylor, "Dispersion of soluble matter in solvent flowing slowly through a tube", *Proc. Roy. Soc. Lond. A* **219** (1953) 186–203.
- [15] S. D. Watt and A. J. Roberts, "The accurate dynamic modelling of dispersion in channels", *SIAM J. Appl. Math.*, to appear.